

Asynchronous control for 2-D Markov jump cyber-physical systems against aperiodic denial-of-service attacks

Peng CHENG¹, Di WU¹, Shuping HE² & Weidong ZHANG^{1*}¹*Department of Automation, Shanghai Jiao Tong University, Shanghai 200240, China;*²*School of Electrical Engineering and Automation, Anhui University, Hefei 230601, China*

Received 3 August 2022/Revised 12 November 2022/Accepted 9 December 2022/Published online 22 May 2023

Abstract This work focuses on the asynchronous controller design for two-dimensional Markov jump cyber-physical systems against denial-of-service attacks. Firstly, due to the openness of the network, it is vulnerable to cyber-attacks, resulting in the control input signal may not being sent to the designated location. Meanwhile, considering the influence of transmission delays and unavoidable packet dropout, a hidden Markov model can help to deal with the unavoidable asynchronous phenomenon between the plant mode and the controller mode. Then, by introducing the concepts of time instants and global states into two-dimensional systems, an asynchronous control scheme for two-dimensional Markov jump cyber-physical systems is successfully formulated. Subsequently, recurring to the multi-Lyapunov function method and iterative technology, sufficient conditions are achieved to make sure that the dynamic hidden two-dimensional Markov jump cyber-physical systems are asymptotically mean-square stable. To conclude, an application example related to the metal rolling process is provided to illustrate the feasibility and effectiveness of the presented asynchronous control scheme under aperiodic denial-of-service attacks.

Keywords asynchronous, two-dimensional, Markov jump cyber-physical systems, denial-of-service attacks, hidden Markov model

Citation Cheng P, Wu D, He S P, et al. Asynchronous control for 2-D Markov jump cyber-physical systems against aperiodic denial-of-service attacks. *Sci China Inf Sci*, 2023, 66(7): 172204, <https://doi.org/10.1007/s11432-022-3660-1>

1 Introduction

With the increasingly close integration of control, communication, and computation, cyber-physical systems (CPSs) have aroused a wide range of research interest in the past decade [1–3]. CPSs are widespread in many engineering applications, such as device interconnection, IoT sensing, smart home, robotics and intelligent navigation [4–6]. Recently, given the vulnerability of CPSs to malicious attacks, there has been an extensive discussion on the security of CPSs. Although some targeted methods have been proposed, for example, information encryption technology [7], it is still not enough to guarantee the reliability of CPSs in the face of attacks from physical equipment or the interaction between the physical layer and the network layer. Therefore, it is critical to study the safety of CPSs from the system perspective.

Currently, CPSs are mainly subject to two common attacks, namely deception attacks and denial-of-service (DoS) attacks. Deception attacks, including fake data injection attacks and replay attacks, modify the transmitted information such that the control unit receives misleading data. As a more accessible form of attack, DoS attacks aim to disrupt data communication between system devices. Then the real-time data will not be sent to the intended destination. Various research efforts have been made on DoS attacks recently. For a class of power systems against DoS attacks, the authors in [8] proposed a distributed resilient filter, which can embody the role of DoS attacks. When DoS attacks are generated by multiple attackers, the authors in [9] constructed a fully distributed frame to analyze the cooperative behavior of multi-agent systems. When considering that DoS attacks would destruct each channel independently, the

* Corresponding author (email: wzhang@sjtu.edu.cn)

authors in [10] designed a decentralized event-triggered controller in accordance with the balance between transmission and tolerable attack strength.

In recent years, two-dimensional (2-D) systems have been active in the research of control theory, which can be used to describe and analyze dynamical systems that evolve in two independent directions, e.g., water splitting [11], image filtering [12], and information communication [13]. Roesser model and Fornasini-Marchesini (FM) model are the most familiar 2-D form, whose developments can be founded in [14]. Note that the strategies on stability analysis [15], sliding mode control [16], and fault detection [17] are all for one-dimensional (1-D) systems, and cannot be capable of applying unchangeably to 2-D systems with higher dimensionality. For this reason, researchers have reported many research achievements on control/filtering for 2-D systems, e.g., [18–22] and the references therein. Considering that 2-D systems may be affected by parameter changes and abrupt structures, the authors in [23–25] injected Markov jump systems (MJSs) into the 2-D system, which is more relevant to the actual engineering. An H_∞ model approximation approach for 2-D MJSs was presented in [23], although the mode information of MJSs may be unknown. In [24], a stability criterion for 2-D MJSs was obtained, in which the Markov chain is inhomogeneous. Based on certain performance levels, a scheme of fault detection and control for 2-D MJSs was achieved in [25]. However, as a whole, 2-D MJSs have not been analyzed thoroughly yet, and still deserve further exploration.

Note that the results in [23–25] for MJSs are in line with the assumption that the controller/filter can accurately acquire the system mode information. Unfortunately, some unfavorable factors, such as time-delays, quantization, and data loss, can result in an asynchronous phenomenon between controller modes and system modes. To overcome this challenge, the authors in [26] designed a mode-independent controller by neglecting all mode information, despite some valuable. Further, Costa et al. [27] raised to form a hidden Markov model (HMM) by releasing a detector to estimate the mode information of the system. The mode relationship between the system and the controller/filter is described by some conditional transitional probabilities. Thanks to this model, the asynchronous quantized sampled-data control issue for fuzzy nonlinear MJSs was solved in [28]. For devising an asynchronous fault detection filter for piecewise homogeneous MJSs, a dual HMM was proposed in [29]. For 2-D MJSs, the control and filtering issues were discussed in [30–33]. However, to the authors' best knowledge, until now, the topic of asynchronous control/filtering for 2-D Markov jump cyber-physical systems (MJCPSS) against DoS attacks has not received enough attention, which triggers the present work.

Based on the above discussion and analysis, this paper intends to investigate the asynchronous control issue for 2-D MJCPSS, whose dynamics develop in two independent directions. Simultaneously, 2-D MJCPSS are suffering from aperiodic DoS attacks. This seems to be hard work and the main difficulties are as follows: (1) How to construct a global state of the 2-D FM local state space model (FMLSSM)? (2) How to reflect the frequency and duration of DoS attacks in the 2-D FMLSSM with two independent directions? (3) How to design an asynchronous control law under DoS attacks? In this paper, we will systematically study these difficulties and give convincing answers.

In this article, the asynchronous controller design issue for 2-D MJCPSS against aperiodic DoS attacks will be investigated. The main bright spots of this article are outlined as follows:

(1) According to the concept of the time instant κ in 2-D systems, we introduce global state X_κ to collect all local states $x_{i,j}$. And then, the frequency and duration of DoS attacks for 2-D MJCPSS can be effectively described.

(2) Thanks to HMM, the mode information of 2-D MJCPSS can be detected by some conditional probabilities. Then, the asynchronous problem between the plant and the controller can be effectively solved.

(3) By the multi-Lyapunov function method and iterative technology, sufficient conditions are achieved to make the dynamic hidden 2-D MJCPSS asymptotically mean-square stable (AMSS).

Notation. In this article, “diag{·}” signifies a block diagonal matrix. \mathcal{N}_1 and \mathcal{N}_2 represent positive integer sets. The symbol $*$ means an ellipsis for terms induced for symmetry. The shorthand $\|\cdot\|$ stands for the Euclidean norm of a vector or its induced matrix norm. $\lambda_{\max}\{M\}$ and $\lambda_{\min}\{M\}$ denote the maximal and minimal eigenvalue matrix M , respectively. $\mathbb{E}\{\cdot\}$ denotes the mathematical expectation.

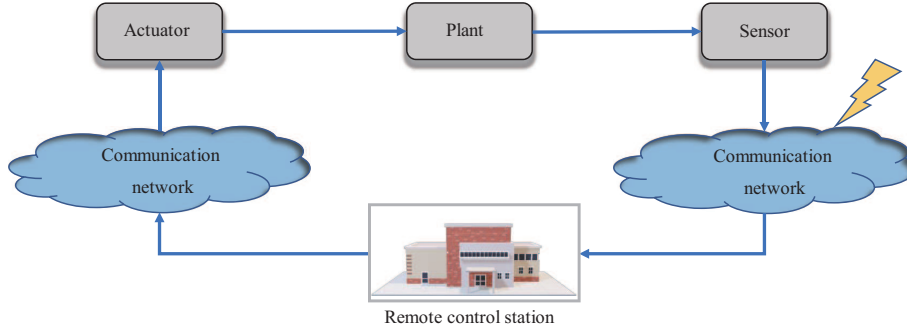


Figure 1 (Color online) The diagram for 2-D MJCPSs under DoS attacks.

2 System description and preliminaries

2.1 System description

As exhibited in Figure 1, the diagram for 2-D MJCPSs under DoS attacks covers a physical plant, a sensor, an actuator, and a remote control station. 2-D MJCPSs outsource their complex computational work to the remote control station. And the signal transmission from the plant to the remote control station is carried out by a communication network, which may suffer from unexpected DoS attacks. In this paper, we consider the following 2-D MJCPSs constructed by an FM model [34]:

$$x_{i+1,j+1} = A_1(r_{i,j+1})x_{i,j+1} + A_2(r_{i+1,j})x_{i+1,j} + B_1(r_{i,j+1})u_{i,j+1} + B_2(r_{i+1,j})u_{i+1,j}, \quad (1)$$

where $x_{i,j} \in \mathbb{R}^q$ is the local state vector, and $u_{i,j} \in \mathbb{R}^p$ is the controlled input. The Markov parameter $r_{i,j}$ takes values in the finite set $\mathcal{N}_1 = \{1, 2, \dots, N_1\}$ with the transition probability matrix $\Lambda = [\sigma_{mn}]$. The jump $r_{i,j}$ is subject to

$$\begin{aligned} \sigma_{mn} &= \Pr(r_{i+1,j+1} = n \mid r_{i,j+1} = m) \\ &= \Pr(r_{i+1,j+1} = n \mid r_{i+1,j} = m) \end{aligned} \quad (2)$$

with $\sigma_{mn} \in [0, 1]$ and $\sum_{n=1}^{N_1} \sigma_{mn} = 1 \forall m, n \in \mathcal{N}_1$. Under $r_{i,j+1} = m$ or $r_{i+1,j} = m$, $A_1(r_{i,j+1})$, $A_2(r_{i+1,j})$, $B_1(r_{i,j+1})$ and $B_2(r_{i+1,j})$ can be abbreviated to A_{1m} , A_{2m} , B_{1m} and B_{2m} .

Let $\bar{x}_{i,j} = [x_{i,j+1}^T \ x_{i+1,j}^T]^T$, $\bar{u}_{i,j} = [u_{i,j+1}^T \ u_{i+1,j}^T]^T$. Then, 2-D MJCPSs (1) equal

$$x_{i+1,j+1} = \bar{A}_m \bar{x}_{i,j} + \bar{B}_m \bar{u}_{i,j}, \quad (3)$$

where $\bar{A}_m = [A_{1m} \ A_{2m}]$, $\bar{B}_m = [B_{1m} \ B_{2m}]$.

As depicted in Figure 2, relative to 1-D systems, the main distinction of 2-D systems is that their information is transmitted in two independent directions. According to this structural characteristic, let X_κ denote the global state, which collects all local states $x_{i,j}$ along the diagonal line $L_\kappa = (i, j) : i + j = \kappa$, that is

$$X(\kappa) = \{x_{i,j} : i + j = \kappa\}. \quad (4)$$

Remark 1. As shown in Figure 2, the global state X_κ collects all the local states $x_{i,j}$ on the diagonal line L_κ . Besides, the evolution of 2-D MJCPSs (1) exhibits that the local state $x_{i+1,j+1}$ results from a global state assignment $x_{i,j+1}$ and $x_{i+1,j}$. Consequently, an increment depending on the global instant κ will be causally imposed on 2-D MJCPSs (1).

The boundary condition (Ξ_0, Γ_0) of 2-D MJCPSs (1) is given as

$$\begin{cases} \Xi_0 = \{x_{0,j}, x_{i,0} \mid i, j = 0, 1, 2, \dots\}, \\ \Gamma_0 = \{r_{0,j}, r_{i,0} \mid i, j = 0, 1, 2, \dots\}. \end{cases} \quad (5)$$

Assumption 1 ([35, 36]). The boundary condition (Ξ_0, Γ_0) is assumed to comply with

$$\lim_{N \rightarrow \infty} \mathbb{E} \left\{ \sum_{\iota=0}^N \left(\|x_{0,\iota}\|^2 + \|x_{\iota,0}\|^2 \right) \right\} < \infty. \quad (6)$$

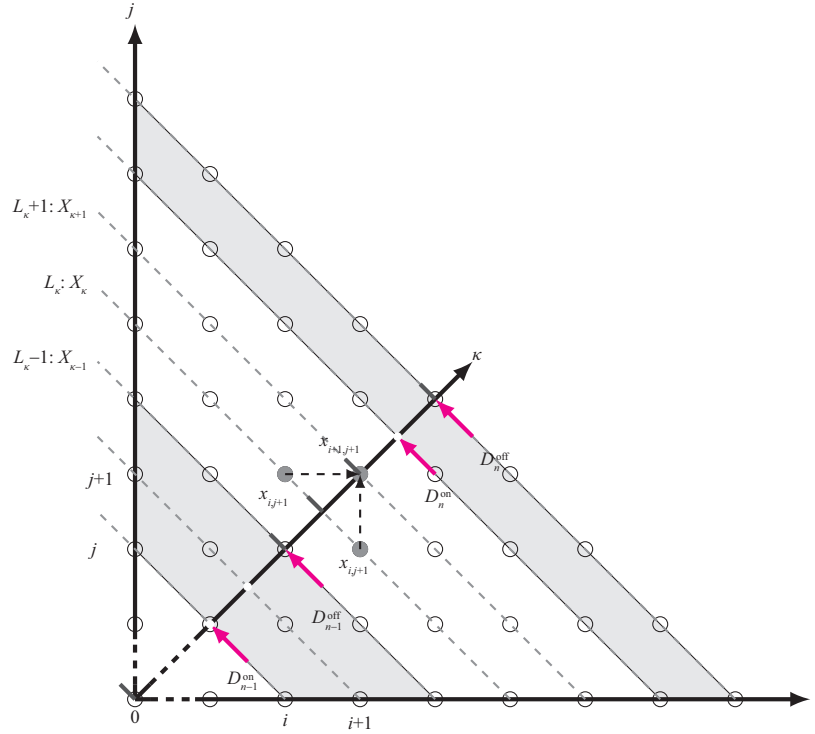


Figure 2 (Color online) Discrete-time 2-D FMLSSM and global state X_k under DoS attacks.

2.2 DoS attacks description

Let $\Delta(a, \kappa)$ represent the times of DoS off/on transitions and $\nabla(a, \kappa)$ denote the total duration in the interval $[a, \kappa)$. To describe DoS attacks, referring to [37], two assumptions are listed to portray the energy bounded property of the concerned DoS attacks.

Assumption 2 (DoS frequency). Over the interval $[a, \kappa)$, there exist scalars $\rho \geq 0$ and $\phi > 0$ satisfying

$$\Delta(a, \kappa) \leq \rho + \frac{\kappa - a}{\phi}. \tag{7}$$

Assumption 3 (DoS duration). Over the interval $[a, \kappa)$, there exist scalars $\lambda \geq 0$ and $\beta > 1$ satisfying

$$\nabla(a, \kappa) \leq \lambda + \frac{\kappa - a}{\beta}. \tag{8}$$

Remark 2. There are two main reasons for the limited energy of DoS attacks. One is that the capability of attackers is limited, and the other is that if the system is always subject to uninterrupted DoS attacks, the controller/filter cannot get any useful data, and then the stability research for the system will be meaningless. Thus, in this paper, two assumptions related to DoS frequency and DoS duration are given to portray the energy-bounded property of DoS attacks. The formulation of Assumption 2 is borrowed from the concept of the average sojourn time in switching systems. Apart from the DoS frequency, we also have to limit the DoS duration, i.e., the length of the intervals over which communication is broken off. Assumption 3 provides a quite natural counterpart to Assumption 2 in terms of DoS duration. Limited energy generated by DoS attacks not only makes controller design and synthesis meaningful, but also has a practical motivation.

2.3 Asynchronous 2-D controller design under DoS attacks

Malicious cyber-attacks may present in the information transfer process because of the openness characteristic of networks, which interrupt communication channels. As depicted in Figure 2, the concerned DoS attacks in this paper are not periodic and the active time of that is designated by $[D_n^{on}, D_n^{off})$, $n \in \mathbb{N}^+$. Obviously, due to the intervention of DoS attacks, the network transmission at the global instants $\kappa - 3$, $\kappa - 2$, $\kappa + 1$ will be invalid and no information can be sent to the controller unit.

Here, we employ variable $\alpha(\kappa)$ to characterize DoS attacks. Then, the asynchronous 2-D controller is specifically presented as

$$\bar{u}_{i,j} = \alpha(\kappa)K_q\bar{x}_{i,j}, \tag{9}$$

where $\alpha(\kappa) = \begin{cases} 0, \kappa \in [D_n^{\text{on}}, D_n^{\text{off}}] \\ 1, \text{others} \end{cases}$ with $\kappa = i + j$ and $K_q = \text{diag}\{K_1(\varphi_{i,j+1}), K_2(\varphi_{i+1,j})\}$. Variable $\varphi_{i,j}$ has a similar feature as variable $r_{i,j}$, taking values in $\mathcal{N}_2 = \{1, 2, \dots, N_2\}$ and satisfying the conditional probability matrix $\bar{\delta} = [\delta_{mq}]$ with

$$\begin{aligned} & \text{Prob}\{\varphi_{i,j+1} = q | r_{i,j+1} = m\} \\ &= \text{Prob}\{\varphi_{i+1,j} = q | r_{i+1,j} = m\} \\ &= \delta_{mq}, \end{aligned} \tag{10}$$

where $\delta_{mq} \in [0, 1]$ and $\sum_{q=1}^{N_2} \delta_{mq} = 1 \forall m \in \mathcal{N}_1, q \in \mathcal{N}_2$.

Under $\varphi_{i,j+1} = q$ or $\varphi_{i+1,j} = q$, the dynamic hidden 2-D MJCPs are derived as

$$x_{i+1,j+1} = \mathcal{A}_{mq}\bar{x}_{i,j}, \tag{11}$$

where $\mathcal{A}_{mq} = \bar{A}_m + \alpha(\kappa)\bar{B}_mK_q$.

2.4 Problem of interest

Definition 1 ([35,36]). The dynamic hidden 2-D MJCPs (11) are said to be AMSS, if, for every initial condition (Ξ_0, Γ_0) satisfying Assumption 1, it has

$$\lim_{i+j \rightarrow \infty} \mathbb{E}\|x(i, j)\|^2 = 0. \tag{12}$$

3 Main results

In this part, some sufficient conditions will be provided to make the dynamic hidden 2-D MJCPs (11) AMSS.

Theorem 1. For given scalars $\rho \geq 0, \lambda \geq 0, \phi > 0, \beta > 1$, the dynamic hidden 2-D MJCPs (11) are AMSS, if there exist $\varrho \geq 1, 0 < \pi_1 < 1, \pi_2 \geq 0, \bar{\pi}_3 > 1 - \pi_1$ and symmetric matrices $P_m > 0, W_m > 0, K_{1q}, K_{2q} \forall m, n \in \mathcal{N}_1, \forall q \in \mathcal{N}_2$, such that the following inequalities hold:

$$\begin{bmatrix} -\bar{\pi}_1\bar{P}_m & \Psi_{1mq} \\ * & \Psi_{2m} \end{bmatrix} < 0, \tag{13}$$

$$\begin{bmatrix} -\bar{\pi}_2\bar{W}_m & \Psi_{3mq} \\ * & \Psi_{4m} \end{bmatrix} < 0, \tag{14}$$

$$\bar{P}_m < \varrho\bar{W}_m, \tag{15}$$

$$\bar{W}_m < \varrho\bar{P}_m, \tag{16}$$

$$0 < \frac{\ln \bar{\pi}_2 - \ln \bar{\pi}_3}{-\ln \bar{\pi}_1 + \ln \bar{\pi}_3} < \beta - 1, \tag{17}$$

$$\ln \bar{\pi}_3 + \frac{\ln \varrho}{\phi} < 0, \tag{18}$$

where

$$\begin{aligned} & \bar{\pi}_1 = 1 - \pi_1, \quad \bar{\pi}_2 = 1 + \pi_2, \\ & \Psi_{1mq} = [\sqrt{\delta_{m1}}\mathcal{A}'_{m1} \sqrt{\delta_{m2}}\mathcal{A}'_{m2} \cdots \sqrt{\delta_{mN_2}}\mathcal{A}'_{mN_2}], \quad \Psi_{2m} = -\text{diag}\{\underbrace{P_m, P_m, \dots, P_m}_{N_2}\}, \end{aligned}$$

$$\Psi_{3mq} = [\sqrt{\delta_{m1}}\mathcal{A}''_{m1} \sqrt{\delta_{m2}}\mathcal{A}''_{m2} \cdots \sqrt{\delta_{mN_2}}\mathcal{A}''_{mN_2}], \quad \Psi_{4m} = -\text{diag}\{\underbrace{\mathcal{W}_m, \mathcal{W}_m, \dots, \mathcal{W}_m}_{N_2}\},$$

$$\mathcal{A}'_{mq} = \bar{A}_m + \bar{B}_m K_q, \quad \mathcal{A}''_{mq} = \bar{A}_m, \quad P_m = \frac{1}{2} \left(\sum_{n=1}^{N_1} \sigma_{mn} P_n \right)^{-1}, \quad \mathcal{W}_m = \frac{1}{2} \left(\sum_{n=1}^{N_1} \sigma_{mn} W_n \right)^{-1},$$

$$\bar{P}_m = \text{diag}\{P_m, P_m\}, \quad \bar{W}_m = \text{diag}\{W_m, W_m\}.$$

Proof. Firstly, we consider the case where no DoS attack occurs. The Lyapunov function for the dynamic hidden 2-D MJCPSs (11) at global instant κ is provided as

$$V_{\alpha_1}(\kappa) = \bar{x}_{i,j}^T \bar{P}_m \bar{x}_{i,j}, \quad \kappa = i + j. \tag{19}$$

For the next global instant $\kappa + 1$, it has

$$V_{\alpha_1}(\kappa + 1) = x_{i+1,j+1}^T \tilde{P}_m x_{i+1,j+1}, \tag{20}$$

where $\tilde{P}_m = 2P_m$.

Following the trajectories of the dynamic hidden 2-D MJCPSs renders

$$\begin{aligned} \Delta V_{\alpha_1}(\kappa) &= V_{\alpha_1}(\kappa + 1) - V_{\alpha_1}(\kappa) \\ &= x_{i+1,j+1}^T \tilde{P}_m x_{i+1,j+1} - \bar{x}_{i,j}^T \bar{P}_m \bar{x}_{i,j}. \end{aligned} \tag{21}$$

For $0 < \pi_1 < 1$, we define

$$\begin{aligned} \mathcal{J}_1 &= \mathbb{E}\{\Delta V_{\alpha_1}(\kappa) + \pi_1 V_{\alpha_1}(\kappa)\} \\ &= \sum_{n=1}^{N_1} \sigma_{mn} \sum_{q=1}^{N_2} \delta_{mq} \{x_{i+1,j+1}^T \tilde{P}_m x_{i+1,j+1}\} + (\pi_1 - 1) \bar{x}_{i,j}^T \bar{P}_m \bar{x}_{i,j}. \end{aligned} \tag{22}$$

Form condition (13), we know $\mathcal{J}_1 < 0$, which means

$$\mathbb{E}\{\Delta V_{\alpha_1}(\kappa)\} < -\pi_1 \mathbb{E}\{V_{\alpha_1}(\kappa)\}. \tag{23}$$

Notice that inequality (11) can only be guaranteed if no DoS attack appears. Then, we move on to discuss the case where the dynamic hidden 2-D MJCPSs (11) suffer from DoS attacks. The Lyapunov function is given as

$$V_{\alpha_0}(\kappa) = \bar{x}_{i,j}^T \bar{W}_m \bar{x}_{i,j}, \quad \kappa = i + j. \tag{24}$$

Similarly, for $\pi_2 \geq 0$, we have

$$\begin{aligned} \mathcal{J}_2 &= \mathbb{E}\{\Delta V_{\alpha_0}(\kappa) - \pi_2 V_{\alpha_0}(\kappa)\} \\ &= \sum_{n=1}^{N_1} \sigma_{mn} \sum_{q=1}^{N_2} \delta_{mq} \{x_{i+1,j+1}^T \tilde{W}_m x_{i+1,j+1}\} - (\pi_2 + 1) \bar{x}_{i,j}^T \bar{W}_m \bar{x}_{i,j}. \end{aligned} \tag{25}$$

Condition (14) can ensure $\mathcal{J}_2 < 0$, that is,

$$\mathbb{E}\{\Delta V_{\alpha_0}(\kappa)\} < \pi_2 \mathbb{E}\{V_{\alpha_0}(\kappa)\}. \tag{26}$$

Let $V(\kappa) = V_{\alpha_1}(\kappa)$ when no DoS attack arises; if not, $V(\kappa) = V_{\alpha_0}(\kappa)$. Next, we set out to analyze the relationships between $V(\kappa)$ and $V(0) \forall \kappa \geq 0$.

Keeping inequalities (23) and (26) in mind, one has

$$\mathbb{E}\{V_{\alpha_1}(\kappa + 1)\} < \bar{\pi}_1 \mathbb{E}\{V_{\alpha_1}(\kappa)\}, \tag{27}$$

$$\mathbb{E}\{V_{\alpha_0}(\kappa + 1)\} < \bar{\pi}_2 \mathbb{E}\{V_{\alpha_0}(\kappa)\}. \tag{28}$$

Besides, conditions (15) and (16) can derive

$$\mathbb{E}\{V_{\alpha_1}(\kappa)\} < \varrho \mathbb{E}\{V_{\alpha_0}(\kappa)\}, \tag{29}$$

$$\mathbb{E}\{V_{\alpha_0}(\kappa)\} < \varrho \mathbb{E}\{V_{\alpha_1}(\kappa)\}. \tag{30}$$

Under DoS attacks, it yields from inequalities (27)–(30) that

$$\begin{aligned} \mathbb{E}\{V(\kappa)\} &< \bar{\pi}_2 \mathbb{E}\{V_{\alpha_0}(\kappa - 1)\} \\ &< \bar{\pi}_2^2 \mathbb{E}\{V_{\alpha_0}(\kappa - 2)\} \\ &\vdots \\ &< \bar{\pi}_2^{\kappa - D_n^{\text{on}}} \mathbb{E}\{V_{\alpha_0}(D_n^{\text{on}})\} \\ &< \bar{\pi}_2^{\kappa - D_n^{\text{on}}} \varrho \mathbb{E}\{V_{\alpha_1}(D_n^{\text{on}})\} \\ &< \bar{\pi}_2^{\kappa - D_n^{\text{on}}} \bar{\pi}_1 \varrho \mathbb{E}\{V_{\alpha_1}(D_n^{\text{on}} - 1)\} \\ &\vdots \\ &< \bar{\pi}_1^{\kappa - \nabla(0, \kappa)} \bar{\pi}_2^{\nabla(0, \kappa)} \varrho^{\Delta(0, \kappa)} V(0). \end{aligned} \tag{31}$$

On the other hand, for $\kappa \notin [D_n^{\text{on}}, D_n^{\text{off}})$, the identical result as inequality (31) can be derived, and the details are omitted here. Then, from inequality (31), we get

$$\begin{aligned} \mathbb{E}V(\kappa) &< \bar{\pi}_1^{\kappa - \nabla(0, \kappa)} \bar{\pi}_2^{\nabla(0, \kappa)} \varrho^{\Delta(0, \kappa)} V(0) \\ &= e^{(\kappa - \nabla(0, \kappa)) \ln \bar{\pi}_1 + \nabla(0, \kappa) \ln \bar{\pi}_2 + \Delta(0, \kappa) \ln \varrho} \\ &< e^{(\kappa - \nabla(0, \kappa)) \ln \bar{\pi}_1 + \nabla(0, \kappa) \ln \bar{\pi}_2 + (\rho + \frac{\kappa}{\phi}) \ln \varrho}. \end{aligned} \tag{32}$$

In the light of Assumption 3, one has

$$\begin{aligned} &(\kappa - \nabla(0, \kappa)) \ln \bar{\pi}_1 + \nabla(0, \kappa) \ln \bar{\pi}_2 \\ &\leq \left(\kappa - \lambda - \frac{\kappa}{\beta}\right) \ln \bar{\pi}_1 + \left(\lambda + \frac{\kappa}{\beta}\right) \ln \bar{\pi}_2 \\ &= \lambda (\ln \bar{\pi}_2 - \ln \bar{\pi}_1) + \kappa \left[\left(1 - \frac{1}{\beta}\right) \ln \bar{\pi}_1 + \frac{1}{\beta} \ln \bar{\pi}_2\right]. \end{aligned} \tag{33}$$

By means of condition (17), it yields

$$\ln \bar{\pi}_2 < -(\beta - 1) \ln \bar{\pi}_1 + \beta \ln \bar{\pi}_3, \tag{34}$$

that is,

$$\left(1 - \frac{1}{\beta}\right) \ln \bar{\pi}_1 + \frac{1}{\beta} \ln \bar{\pi}_2 < \ln \bar{\pi}_3. \tag{35}$$

Combining inequality (33) with inequality (35), we acquire

$$(\kappa - \nabla(0, \kappa)) \ln \bar{\pi}_1 + \nabla(0, \kappa) \ln \bar{\pi}_2 < \kappa \ln \bar{\pi}_3 + \lambda (\ln \bar{\pi}_2 - \ln \bar{\pi}_1). \tag{36}$$

Substituting inequality (36) into inequality (32) can render

$$\begin{aligned} \mathbb{E}V(\kappa) &< e^{[\lambda (\ln \bar{\pi}_2 - \ln \bar{\pi}_1) + \rho \ln \varrho]} e^{(\ln \bar{\pi}_3 + \frac{\ln \varrho}{\phi}) \kappa} V(0) \\ &= \frac{\bar{\pi}_2^\lambda \varrho^{\frac{\rho}{\phi}}}{\bar{\pi}_1^\lambda} \left(\bar{\pi}_3 \varrho^{\frac{1}{\phi}}\right)^\kappa V(0). \end{aligned} \tag{37}$$

Let

$$c \mathbb{E}\|x_{i,j}\|^2 \leq \mathbb{E}V(\kappa), \quad V(0) \leq d \|x_{0,0}\|^2, \tag{38}$$

where

$$c = \min \left\{ \min_{m \in N_1} \{\lambda_{\min}\{\bar{P}_m\}\}, \min_{m \in N_1} \{\lambda_{\min}\{\bar{W}_m\}\} \right\},$$

$$d = \max \left\{ \max_{m \in \mathcal{N}_1} \{ \lambda_{\max} \{ \bar{P}_m \} \}, \max_{m \in \mathcal{N}_1} \{ \lambda_{\max} \{ \bar{W}_m \} \} \right\}.$$

Inequalities (37) and (38) lead to

$$\mathbb{E} \|x_{i,j}\|^2 < \frac{d \bar{\pi}_2^\lambda \varrho^{\frac{\rho}{\pi}}}{c \bar{\pi}_1^\lambda} \left(\bar{\pi}_3 \varrho^{\frac{1}{\phi}} \right)^\kappa \|x_{0,0}\|^2. \tag{39}$$

From inequality (18), we have $\bar{\pi}_3 \varrho^{\frac{1}{\phi}} < 1$, which together with (39) and Assumption 1 implies that $\mathbb{E} \|x_{i,j}\|^2 \rightarrow 0$ as $\kappa \rightarrow \infty$. Then, the dynamic hidden 2-D MJCPSs (11) are guaranteed to be AMSS, which ends the proof.

Although some brief conditions are attained in Theorem 1, there exist some nonlinearities which will be a hindrance to the controller design. Therefore, in the following, we will perform linearization to the conditions in Theorem 1.

Theorem 2. For given scalars $\rho \geq 0, \lambda \geq 0, \phi > 0, \beta > 1$, if there exist $\varrho \geq 1, 0 < \pi_1 < 1, \pi_2 \geq 0, \bar{\pi}_3 > 1 - \pi_1$ and positive-definite symmetric matrices $\hat{P}_m, \hat{W}_m, X_{1m}, X_{2m}$, matrices $G_1, G_2, \mathcal{K}_{1\mu}$ and $\mathcal{K}_{2\mu} \forall m, n \in \mathcal{N}_1, \forall q \in \mathcal{N}_2$, such that the following linear matrix inequalities hold:

$$\begin{bmatrix} -X_{1m} & \mathcal{X}_{1m} \\ * & -\mathbb{P}_m \end{bmatrix} < 0, \tag{40}$$

$$\begin{bmatrix} -X_{2m} & \mathcal{X}_{2m} \\ * & -\mathbb{W}_m \end{bmatrix} < 0, \tag{41}$$

$$\tilde{\Omega}_{2 \times 2} < 0, \tag{42}$$

$$\tilde{\Pi}_{2 \times 2} < 0, \tag{43}$$

$$\hat{P}_m < \varrho \hat{W}_m, \tag{44}$$

$$\hat{W}_m < \varrho \hat{P}_m, \tag{45}$$

where

$$\mathcal{X}_{1m} = \left[\sqrt{2\sigma_{m1}} X_{1m}, \sqrt{2\sigma_{m2}} X_{1m}, \dots, \sqrt{2\sigma_{mN_1}} X_{1m} \right],$$

$$\mathcal{X}_{2m} = \left[\sqrt{2\sigma_{m1}} X_{2m}, \sqrt{2\sigma_{m2}} X_{2m}, \dots, \sqrt{2\sigma_{mN_1}} X_{2m} \right],$$

$$\mathbb{P}_m = -\text{diag}\{\hat{P}_1, \hat{P}_2, \dots, \hat{P}_{N_1}\}, \quad \mathbb{W}_m = -\text{diag}\{\hat{W}_1, \hat{W}_2, \dots, \hat{W}_{N_1}\},$$

$$\tilde{\Omega}_{11} = -\bar{\pi}_1 \text{diag}\{G_1^T - \hat{P}_m + G_1, G_1^T - \hat{P}_m + G_1\}, \quad \tilde{\Omega}_{12} = \left[\sqrt{\delta_{m1}} \tilde{\Upsilon}_{1m1} \quad \sqrt{\delta_{m2}} \tilde{\Upsilon}_{1m2} \quad \dots \quad \sqrt{\delta_{mN_2}} \tilde{\Upsilon}_{1mN_2} \right],$$

$$\tilde{\Upsilon}_{1mq} = \begin{bmatrix} G_1^T A_{1m}^T + \mathcal{K}_{1p}^T B_{1m}^T \\ G_1^T A_{2m}^T + \mathcal{K}_{2p}^T B_{2m}^T \end{bmatrix}, \quad \tilde{\Omega}_{22} = -\text{diag}\{\underbrace{X_{1m}, X_{1m}, \dots, X_{1m}}_{N_2}\},$$

$$\tilde{\Pi}_{11} = -\bar{\pi}_2 \text{diag}\{G_2^T - \hat{W}_m + G_2, G_2^T - \hat{W}_m + G_2\}, \quad \tilde{\Pi}_{12} = \left[\delta_{m1} \tilde{\Upsilon}_{2m1} \quad \delta_{m2} \tilde{\Upsilon}_{2m2} \quad \dots \quad \delta_{mN_2} \tilde{\Upsilon}_{2mN_2} \right],$$

$$\tilde{\Upsilon}_{2mq} = \begin{bmatrix} G_2^T A_{1m}^T \\ G_2^T A_{2m}^T \end{bmatrix}, \quad \tilde{\Pi}_{22} = -\text{diag}\{\underbrace{X_{2m}, X_{2m}, \dots, X_{2m}}_{N_2}\},$$

then the dynamic hidden 2-D MJCPSs (11) are guaranteed to be AMSS. In addition, the asynchronous controller gain can be described by $K_{1\mu} = \mathcal{K}_{1\mu} G^{-1}, K_{2\mu} = \mathcal{K}_{2\mu} G^{-1}$.

Proof. First, we prescribe the following relationship:

$$\hat{P}_m = P_m^{-1}, \quad \hat{W}_m = W_m^{-1}, \quad \mathcal{K}_{1\mu} = GK_{1\mu}, \quad \mathcal{K}_{2\mu} = GK_{2\mu}.$$

It yields from condition (40) that $-\mathcal{P}_m < -X_{1m}$. Then, carrying on a congruence transformation to inequality (13) with $\text{diag}\{G, G, \underbrace{I, I, \dots, I}_{N_1}\}$, one has

$$\Omega_{2 \times 2} < 0, \tag{46}$$

where

$$\Omega_{11} = -\bar{\pi}_1 \text{diag}\{G_1^T \hat{P}_m^{-1} G_1, G_1^T \hat{P}_m^{-1} G_1\}, \quad \Omega_{12} = \left[\sqrt{\delta_{m1}} \Upsilon_{1m1} \quad \sqrt{\delta_{m2}} \Upsilon_{1m2} \quad \cdots \quad \sqrt{\delta_{mN_2}} \Upsilon_{1mN_2} \right],$$

$$\Upsilon_{1mq} = \begin{bmatrix} G^T A_{1m}^T + G^T K_{1p}^T B_{1m}^T \\ G^T A_{2m}^T + G^T K_{2p}^T B_{2m}^T \end{bmatrix}, \quad \Omega_{22} = -\text{diag}\{\underbrace{X_{1m}, X_{1m}, \dots, X_{1m}}_{N_2}\}.$$

Keeping $G^T \hat{P}_m^{-1} G \geq G^T - \hat{P}_m + G$ in mind, we know that inequality (40) can be deduced from inequality (13). Similarity, inequality (41) is evolved from inequality (14). Besides, inequalities (15) and (16) are equivalent to inequalities (44) and (45), respectively.

Remark 3. Referring to [38], we know that computational complexity can commonly be characterized by the number of decision variables. In Theorem 1, the number of decision variables is $q(q + 1)N_1 + 2pqN_2 + 4$, where N_1 and N_2 denote the number of system modes and asynchronous controller modes, respectively. However, the restraints in Theorem 1 have some nonlinearities, which are an obstacle to the design of the controller. Theorem 2 is proposed to linearize the restraints in Theorem 1, such that the resultant results can be solved by Matlab linear matrix inequality toolbox, directly. The number of decision variables in Theorem 2 is $5q^2N_1 + 3qN_1 + 2pqN_2 + 4$, which indicates that the results of the linearization of Theorem 2 introduce conservatism due to the increased computational complexity. Therefore, designing an intelligent algorithm to address the nonlinear problem without introducing any conservatism will be one of our next research efforts.

4 Illustrative example

Consider metal rolling process (MRP)-based 2-D MJCPSs shown in Figure 3, where the network layer suffers from DoS attacks, and the physical layer is an MRP. The dynamics of the controlled plant is modeled as [39]

$$l_i(t) = \frac{\bar{\gamma}_m}{\bar{\gamma}_m + Ma^2} \left\{ \left(1 + \frac{Ma^2}{\gamma_{1m}} \right) l_{i-1}(t) - \frac{F_M}{\gamma_2} \right\}, \tag{47}$$

where a denotes the differentiation operator $d/d(t)$, $l_i(t)$ is the i th actual roll-gap thickness, F_M represents the force developed by the motor, M means the lumped mass of the roll-gap adjusting mechanism, γ_{1m} , γ_2 and $\bar{\gamma}_m$ refer to the stiffness of the adjusting mechanism spring, the hardness of the metal strip, and the composite stiffness of the metal strip and the rolling mechanism, respectively.

By adopting a backward difference approach and selecting the sampling period h , MRP (47) can be transformed into

$$l_i(t + h) = d_{1m}l_i(t) + d_{2m}l_i(t - h) + d_{3m}l_{i-1}(t + h) + d_{4m}l_{i-1}(t) + d_{5m}l_{i-1}(t - h) + \theta_m u_i(t) \tag{48}$$

with $d_{1m} = \frac{2M}{\bar{\gamma}_m h^2 + M}$, $d_{2m} = \frac{-M}{\bar{\gamma}_m h^2 + M}$, $d_{3m} = 1$, $d_{4m} = \frac{-2\bar{\gamma}_m M}{\gamma_{1m}(\bar{\gamma}_m h^2 + M)}$, $d_{5m} = \frac{\bar{\gamma}_m M}{\gamma_{1m}(\bar{\gamma}_m h^2 + M)}$, $\theta_m = \frac{-\bar{\gamma}_m h^2}{\gamma_2(\bar{\gamma}_m h^2 + M)}$, $\bar{\gamma}_m = \frac{\gamma_{1m}\gamma_2}{\gamma_{1m} + \gamma_2}$, $m = 1, 2$.

Remark 4. Assume that the stiffness of the adjusting mechanism spring in Figure 3 may suffer from sudden structure change due to long-term use. Fortunately, the Markov jump model is suitable for describing this phenomenon. In this simulation, we consider the stiffness of the adjusting mechanism spring switches stochastically in both cases.

Define $t = jh$, $x_{i,j} \triangleq [l_{i-1}((j + 1)h) \quad l_{i-1}(jh) \quad l_i(jh) \quad l_i((j - 1)h) \quad l_{i-1}((j - 1)h)]^T$, $u_{i,j} \triangleq u_i(t)$, and we can further convert equation (48) to 2-D MJCPSs (1) with

$$A_{1m} = \begin{bmatrix} d_{3m} & d_{4m} & d_{1m} & d_{2m} & d_{5m} \\ 0 & 0 & 1 & 0 & 0 \\ 0 & 0 & 0 & 0 & 0 \\ 0 & 0 & 0 & 0 & 0 \\ 0 & 0 & 0 & 0 & 0 \end{bmatrix}, \quad A_{2m} = \begin{bmatrix} 0 & 0 & 0 & 0 & 0 \\ 0 & 0 & 0 & 0 & 0 \\ d_{3m} & d_{4m} & d_{1m} & d_{2m} & d_{5m} \\ 0 & 0 & 1 & 0 & 0 \\ 0 & 1 & 0 & 0 & 0 \end{bmatrix},$$

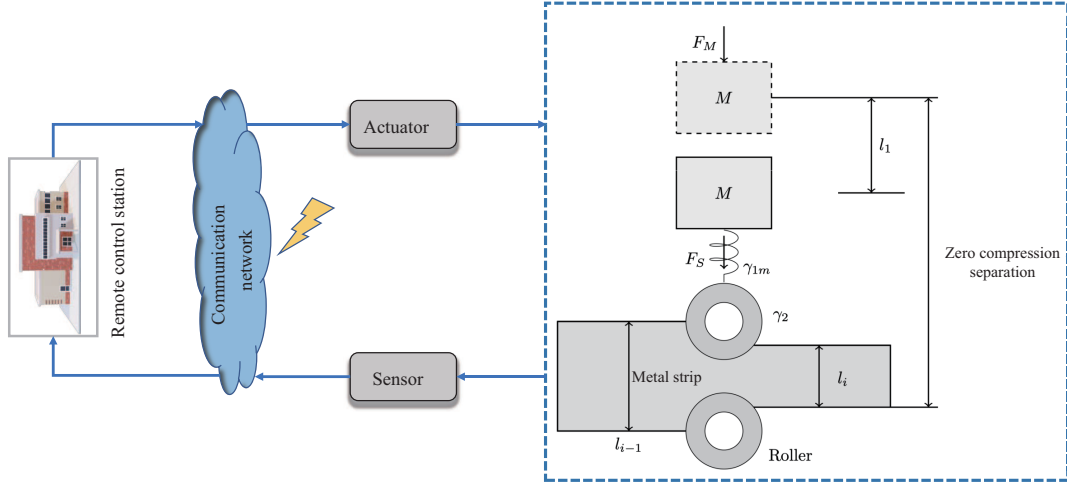


Figure 3 (Color online) The framework of the MRP-based 2-D MJCPSs under DoS attacks.

$$B_{1m} = [\theta_m \ 0 \ 0 \ 0 \ 0]^T, \quad B_{2m} = [0 \ 0 \ \theta_m \ 0 \ 0]^T.$$

Setting $\gamma_{11} = 1000 \text{ N/mm}$, $\gamma_{12} = 3000 \text{ N/mm}$, $\gamma_2 = 500 \text{ N/mm}$, $M = 50 \text{ kg}$ and $h = 1 \text{ s}$, it has Modes 1 and 2.

Mode 1:

$$A_{11} = \begin{bmatrix} 1.0000 & -0.0870 & 0.2609 & -0.1304 & 0.0435 \\ 0 & 0 & 1.0000 & 0 & 0 \\ 0 & 0 & 0 & 0 & 0 \\ 0 & 0 & 0 & 0 & 0 \\ 0 & 0 & 0 & 0 & 0 \end{bmatrix},$$

$$A_{21} = \begin{bmatrix} 0 & 0 & 0 & 0 & 0 \\ 0 & 0 & 0 & 0 & 0 \\ 1.0000 & -0.0870 & 0.2609 & -0.1045 & 0.0435 \\ 0 & 0 & 1.0000 & 0 & 0 \\ 0 & 1.0000 & 0 & 0 & 0 \end{bmatrix},$$

$$B_{11} = [-0.0017 \ 0 \ 0 \ 0 \ 0]^T, \quad B_{21} = [0 \ 0 \ -0.0017 \ 0 \ 0]^T.$$

Mode 2:

$$A_{12} = \begin{bmatrix} 1.0000 & -0.0299 & 0.2090 & -0.1045 & 0.0149 \\ 0 & 0 & 1.0000 & 0 & 0 \\ 0 & 0 & 0 & 0 & 0 \\ 0 & 0 & 0 & 0 & 0 \\ 0 & 0 & 0 & 0 & 0 \end{bmatrix},$$

$$A_{22} = \begin{bmatrix} 0 & 0 & 0 & 0 & 0 \\ 0 & 0 & 0 & 0 & 0 \\ 1.0000 & -0.0299 & 0.2090 & -0.1045 & 0.0149 \\ 0 & 0 & 1.0000 & 0 & 0 \\ 0 & 1.0000 & 0 & 0 & 0 \end{bmatrix},$$

$$B_{21} = [0 \ 0 \ -0.0018 \ 0 \ 0]^T, \quad B_{22} = [-0.0018 \ 0 \ 0 \ 0 \ 0]^T.$$

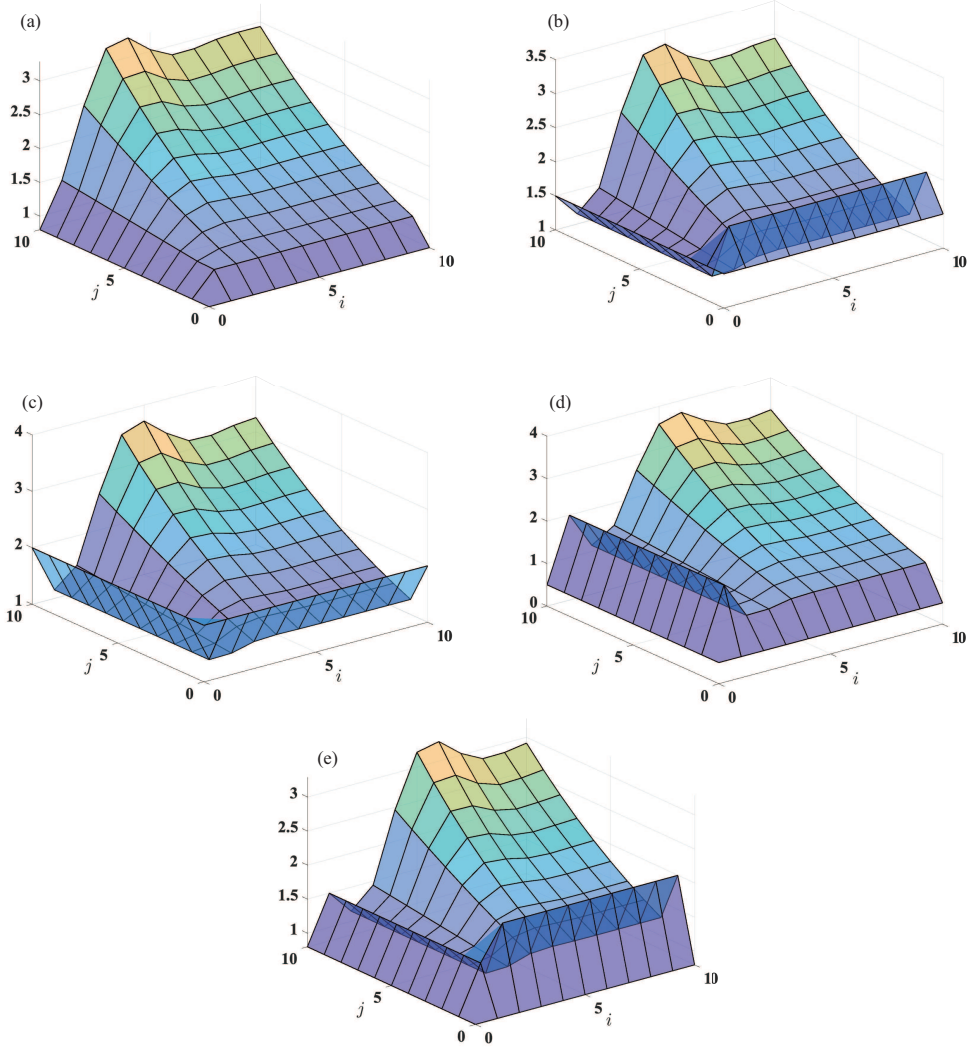


Figure 4 (Color online) State trajectory $x_{i,j}$ in the open-loop case. (a) x_{1ij} ; (b) x_{2ij} ; (c) x_{3ij} ; (d) x_{4ij} ; (e) x_{5ij} .

The transition probability matrix Λ and the conditional probability matrix $\bar{\delta}$ are given as

$$\Lambda = \begin{bmatrix} 0.3 & 0.7 \\ 0.6 & 0.4 \end{bmatrix}, \quad \bar{\delta} = \begin{bmatrix} 0.4 & 0.6 \\ 0.8 & 0.2 \end{bmatrix}.$$

In addition, we set $\rho = 5$, $\lambda = 5$, $\phi = 2$ and $\beta = 3$ to construct DoS attacks, and set $\varrho = 1$, $\pi_1 = 0.01$, $\pi_2 = 0.08$ and $\bar{\pi}_3 = 1.02$ to satisfy conditions (17) and (18). By solving linear matrix inequalities (40)–(45), we have

Mode 1:

$$K_{11} = \begin{bmatrix} 563.6834 & -27.9471 & 128.4638 & -64.1090 & 14.1515 \end{bmatrix},$$

$$K_{21} = \begin{bmatrix} 561.2206 & -25.8543 & 126.8595 & -58.9354 & 8.7069 \end{bmatrix};$$

Mode 2:

$$K_{12} = \begin{bmatrix} 568.7185 & -38.0541 & 136.4158 & -69.1605 & 19.2047 \end{bmatrix},$$

$$K_{22} = \begin{bmatrix} 565.6775 & -30.5889 & 134.4258 & -60.0817 & 9.5221 \end{bmatrix}.$$

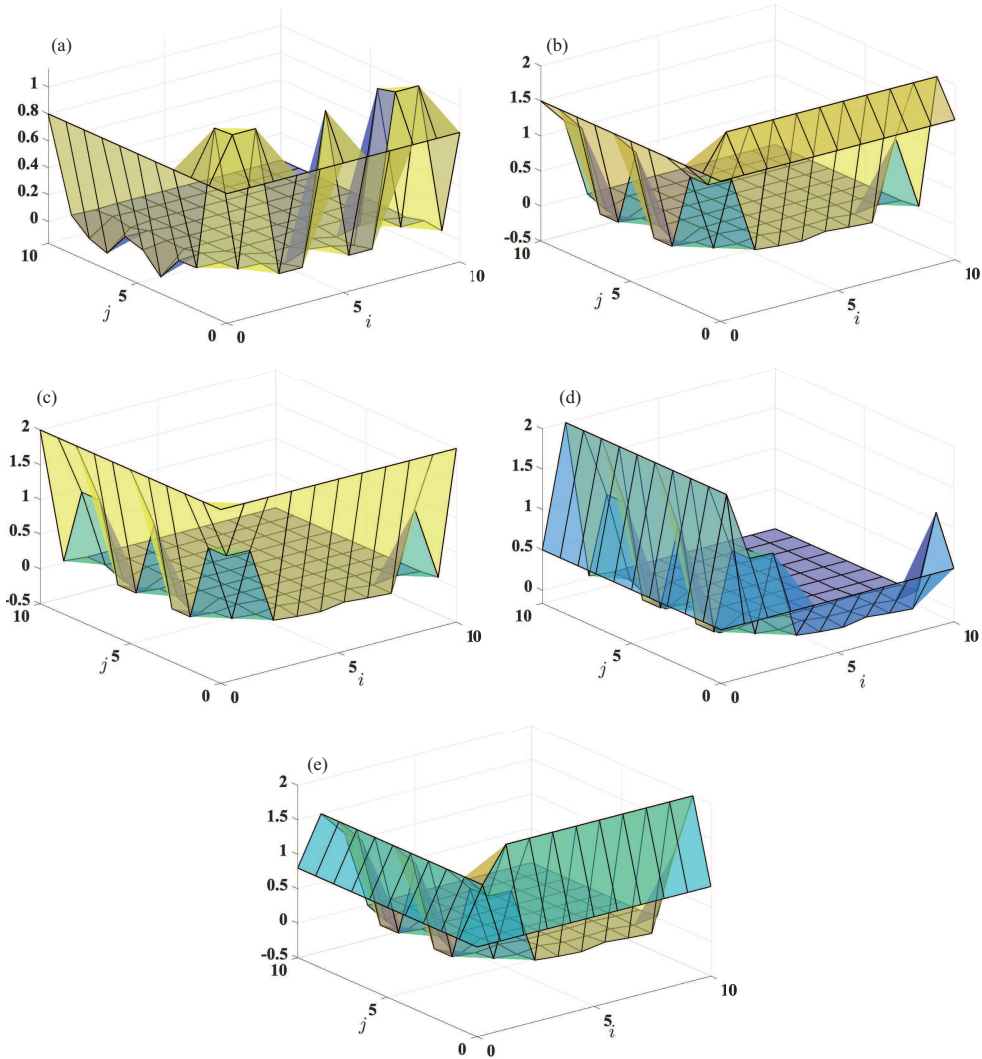


Figure 5 (Color online) State trajectory $x_{i,j}$ in the closed-loop case. (a) x_{1ij} ; (b) x_{2ij} ; (c) x_{3ij} ; (d) x_{4ij} ; (e) x_{5ij} .

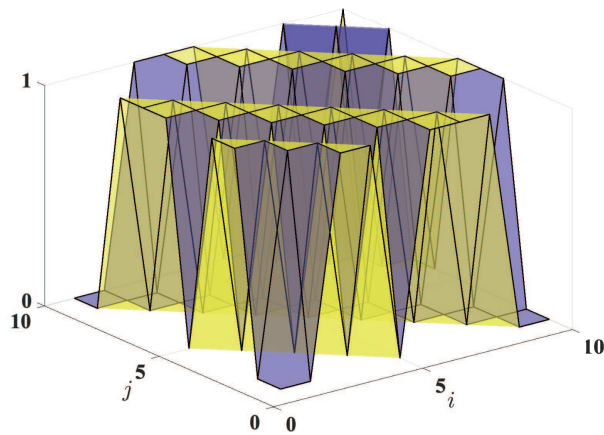


Figure 6 (Color online) Switching mechanism of DoS attacks under Case III.

By doing this, Figure 4 presents the state trajectories of 2-D MJCPSs (1) in the absence of control actions, in which the five subfigures indicate that 2-D MJCPSs (1) are not stable. Through the asynchronous 2-D controller (9), the state trajectories of the dynamic hidden 2-D MJCPSs (11) are shown in Figure 5, which suggests that the concerned system is AMSS, although the DoS attacks portrayed in

Table 1 Comparison of system stability performance under five DoS attacks

Different case	DoS frequency	E_{SUM}
Case I	$\Delta(0, 20) = 5$	162.0538
Case II	$\Delta(0, 20) = 7$	187.3809
Case III	$\Delta(0, 20) = 9$	197.0091
Case IV	$\Delta(0, 20) = 11$	212.7102
Case V	$\Delta(0, 20) = 13$	235.5337

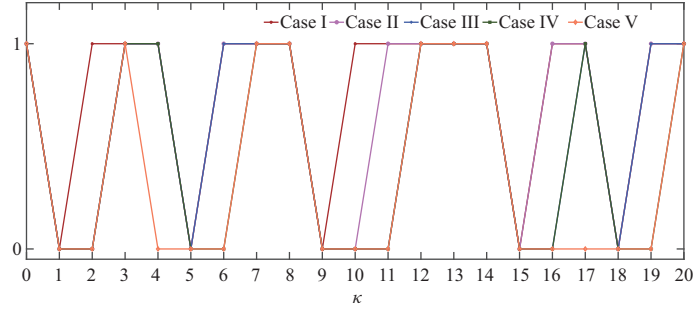
**Figure 7** (Color online) Five different DoS attack sequences.

Figure 6 appear.

Table 1 gives the comparison of system stability performance under five DoS attacks, and the specific sequences of five DoS attacks are provided in Figure 7. It is worth noting that, for the sake of comparison, the frequency of the attacks is only increased from the original. Set $E_{\text{SUM}} = \mathbb{E}\{\|x_{p,q}\|^2\}$ to reflect the quality of system stability. It is not difficult to understand that the smaller the value of E_{SUM} , the better the system stability performance of the system. From Table 1, we can claim that the increase in attack frequency does weaken the stability performance of the system.

Remark 5. Hu et al. [40, 41] utilized parameter T_{off}^{\min} to signify the uniform lower boundedness of the sleeping period in every active period T , resulting in the DoS attacks being periodic. However, attackers may launch cyber attacks from time to time to prevent attacks from being detected or circumvented. The DoS attacks in this article are free from periodicity constraints through frequency and duration description, which are more general than the periodic DoS attacks in [40, 41].

Remark 6. Note that the existing results on DoS attacks in [8–10] are for 1-D systems. Due to the increase in dimensionality, the above conclusions cannot be directly applied to 2-D systems. At present, there are very few studies on the dynamic behavior analysis of 2-D systems under DoS attacks. In this article, we introduce the concepts of instants and global states into 2-D MJCPSs, which can help describe the two constraints of frequency and duration of DoS attacks in 2-D MJCPSs.

5 Conclusion

The objective of this work is to investigate the asynchronous control issue for 2-D MJCPSs suffering from aperiodic DoS attacks. At first, the asynchronous phenomenon between the concerned system and the 2-D controller is carried out by an HMM. Then, the concepts of time instants and global states are introduced into 2-D MJCPSs, which can help to describe the frequency and duration of DoS attacks for 2-D MJCPSs. Subsequently, by the multi-Lyapunov function method and iterative technology, sufficient conditions are achieved to ensure that the dynamic hidden 2-D MJCPSs are AMSS. Finally, we utilize an application example related to the MRP to clarify the feasibility and effectiveness of the proposed asynchronous control scheme under aperiodic DoS attacks.

Acknowledgements This work was partly supported by Hainan Province Science and Technology Special Fund (Grant No. ZDYF2021GXJS041), Key-Area Research and Development Program of Guangdong Province (Grant No. 2020B1111010002), and National Natural Science Foundation of China (Grant No. U2141234).

References

- 1 Zhang Y F, Wu Z-G, Wu Z Z, et al. Resilient observer-based event-triggered control for cyber-physical systems under asynchronous denial-of-service attacks. *Sci China Inf Sci*, 2022, 65: 142203

- 2 Liu L, Zhao X D, Wang B H, et al. Event-triggered state estimation for cyber-physical systems with partially observed injection attacks. *Sci China Inf Sci*, 2023, 66: 169202
- 3 Shen W, Lü X B, Ma C J. Robust force tracking control via backstepping sliding mode control and virtual damping control for hydraulic quadruped robots. *J Cent South Univ*, 2020, 27: 2673–2686
- 4 Gatouillat A, Badr Y, Massot B, et al. Internet of medical things: a review of recent contributions dealing with cyber-physical systems in medicine. *IEEE Internet Things J*, 2018, 5: 3810–3822
- 5 Ding Y D, Wang Y Y, Jiang S R, et al. Active fault-tolerant control scheme of aerial manipulators with actuator faults. *J Cent South Univ*, 2021, 28: 771–783
- 6 Du B, Lin B, Zhang C, et al. Safe deep reinforcement learning-based adaptive control for USV interception mission. *Ocean Eng*, 2022, 246: 110477
- 7 Yang J, Johansson T. An overview of cryptographic primitives for possible use in 5G and beyond. *Sci China Inf Sci*, 2020, 63: 220301
- 8 Chen W, Ding D, Dong H, et al. Distributed resilient filtering for power systems subject to denial-of-service attacks. *IEEE Trans Syst Man Cybern Syst*, 2019, 49: 1688–1697
- 9 Xu W, Hu G, Ho D W C, et al. Distributed secure cooperative control under denial-of-service attacks from multiple adversaries. *IEEE Trans Cybern*, 2019, 50: 3458–3467
- 10 Lu A Y, Yang G H. Observer-based control for cyber-physical systems under denial-of-service with a decentralized event-triggered scheme. *IEEE Trans Cybern*, 2019, 50: 4886–4895
- 11 Faraji M, Yousefi M, Yousefzadeh S, et al. Two-dimensional materials in semiconductor photoelectrocatalytic systems for water splitting. *Energy Environ Sci*, 2019, 12: 59–95
- 12 Wang F, Wang Z, Liang J, et al. A survey on filtering issues for two-dimensional systems: advances and challenges. *Int J Control Autom Syst*, 2020, 18: 629–642
- 13 Wang F, Wang Z, Liang J, et al. Recursive distributed filtering for two-dimensional shift-varying systems over sensor networks under stochastic communication protocols. *Automatica*, 2020, 115: 108865
- 14 Du C, Xie L. H_∞ Control and Filtering of Two-Dimensional Systems. Berlin: Springer, 2002. 278
- 15 Li X, Ho D W C, Cao J. Finite-time stability and settling-time estimation of nonlinear impulsive systems. *Automatica*, 2019, 99: 361–368
- 16 Song J, Wang Z, Niu Y. On H_∞ sliding mode control under stochastic communication protocol. *IEEE Trans Automat Contr*, 2018, 64: 2174–2181
- 17 Jiang X S, Zhao D Y. Event-triggered fault detection for nonlinear discrete-time switched stochastic systems: a convex function method. *Sci China Inf Sci*, 2021, 64: 200204
- 18 Song J, Niu Y. Co-design of 2-D event generator and sliding mode controller for 2-D Roesser model via genetic algorithm. *IEEE Trans Cybern*, 2021, 51: 4581–4590
- 19 Wang M, Qiu J B, Yan H C, et al. Static output feedback control for uncertain Roesser-type continuous-time two-dimensional piecewise affine systems. *Sci China Inf Sci*, 2022, 65: 219204
- 20 Cheng J, Wu Y, Yan H, et al. Protocol-based filtering for fuzzy Markov affine systems with switching chain. *Automatica*, 2022, 141: 110321
- 21 Cheng J, Xie L, Park J H, et al. Protocol-based output-feedback control for semi-Markov jump systems. *IEEE Trans Automat Contr*, 2022, 67: 4346–4353
- 22 Lv X, Niu Y, Park J H, et al. Sliding mode control for 2D FMII systems: a bidirectional dynamic event-triggered strategy. *Automatica*, 2023, 147: 110727
- 23 Wei Y, Qiu J, Karimi H R, et al. Model approximation for two-dimensional Markovian jump systems with state-delays and imperfect mode information. *Multidim Syst Sign Process*, 2015, 26: 575–597
- 24 Dzung N T, Hien L V. Robust stabilization of non-stationary Markov jump 2-D systems with multiplicative noises. *J Franklin Inst*, 2021, 358: 7413–7425
- 25 Li Z, Li Q, Ding D W. Integrated fault detection and control for two-dimensional Markovian jump systems. *Int J Robust Nonlinear Control*, 2019, 29: 5621–5640
- 26 Feng Z, Shi P. Sliding mode control of singular stochastic Markov jump systems. *IEEE Trans Automat Contr*, 2017, 62: 4266–4273
- 27 Costa O L V, Fragoso M D, Todorov M G. A detector-based approach for the H_2 control of Markov jump linear systems with partial information. *IEEE Trans Automat Contr*, 2015, 60: 1219–1234
- 28 Wu T, Xiong L, Cao J, et al. Hidden Markov model-based asynchronous quantized sampled-data control for fuzzy nonlinear Markov jump systems. *Fuzzy Sets Syst*, 2022, 432: 89–110
- 29 Cheng P, Chen M, Stojanovic V, et al. Asynchronous fault detection filtering for piecewise homogenous Markov jump linear systems via a dual hidden Markov model. *Mech Syst Signal Processing*, 2021, 151: 107353
- 30 Zhu J, Li C, Dullerud G E. Asynchronous control for two-dimensional hidden Markovian jump systems with partly known mode observation conditional probabilities. *Int J Robust Nonlinear Control*, 2020, 30: 3344–3364
- 31 Cheng J, Park J H, Yan H, et al. An event-triggered round-robin protocol to dynamic output feedback control for nonhomo-

- geneous Markov switching systems. *Automatica*, 2022, 145: 110525
- 32 Cheng P, He S P, Luan X L, et al. Finite-region asynchronous H_∞ control for 2D Markov jump systems. *Automatica*, 2021, 129: 109590
- 33 Cheng P, Zhang G, Zhang W, et al. Co-design of adaptive event-triggered mechanism and asynchronous H_∞ control for 2-D Markov jump systems via genetic algorithm. *IEEE Trans Cybern*, 2022. doi: 10.1109/TCYB.2022.3169530
- 34 Yang R, Zheng W X. Two-dimensional sliding mode control of discrete-time fornasini-marchesini systems. *IEEE Trans Automat Contr*, 2019, 64: 3943–3948
- 35 Gao H, Lam J, Wang C, et al. Robust H_∞ filtering for 2D stochastic systems. *Circuits Syst Signal Process*, 2004, 23: 479–505
- 36 Wu L, Shi P, Gao H, et al. H_∞ filtering for 2D Markovian jump systems. *Automatica*, 2008, 44: 1849–1858
- 37 De Persis C, Tesi P. Input-to-state stabilizing control under denial-of-service. *IEEE Trans Automat Contr*, 2015, 60: 2930–2944
- 38 Lian Z, He Y, Zhang C K, et al. Stability and stabilization of T-S fuzzy systems with time-varying delays via delay-product-type functional method. *IEEE Trans Cybern*, 2019, 50: 2580–2589
- 39 Yamada M, Xu L, Saito O. 2D model-following servo system. *Multidim Syst Signal Process*, 1999, 10: 71–91
- 40 Hu S, Yue D, Han Q L, et al. Observer-based event-triggered control for networked linear systems subject to denial-of-service attacks. *IEEE Trans Cybern*, 2019, 50: 1952–1964
- 41 Hu S, Yue D, Xie X, et al. Resilient event-triggered controller synthesis of networked control systems under periodic DoS jamming attacks. *IEEE Trans Cybern*, 2018, 49: 4271–4281